JTTEE5 16:839–843
DOI: 10.1007/s11666-007-9081-0
1059-9630/$19.00 © ASM International

On the Role of Spraying Process on Microstructural, Mechanical, and Thermal Response of Alumina Coatings

S. Costil, C. Verdy, R. Bolot, and C. Coddet

(Submitted February 27, 2007; in revised form June 7, 2007)

Thermal spraying is a widely used technology for industrial applications to provide coatings that improve the surface characteristics. According to the specificities of processes (APS, VPS, flame, electric arc), any kind of material can be sprayed. Among materials, ceramic coatings present several interesting aspects such as wear resistance, corrosion protection as well as thermal or electrical insulation; particularly alumina coatings which appear as the most commonly used. From all spraying processes, atmospheric plasma spraying (APS) is a rather well-established process but some others can also be used with a lower economical impact such as the flame technology. The aim of this study was to analyze the alumina coating properties according to the technology employed such as APS or wire flame spraying using the Rokide™ and the Master Jet® guns. After micrographic analyses by SEM, physical and mechanical properties were measured considering the thermal conductivity and the hardness.

Keywords alumina coating, APS, coating characteristics, flame spraying, microstructure, SEM

1. Introduction

Thermal spraying is a widely used technology in a large range of industrial applications to provide coatings that improve the surface characteristics. Whatever the technology used, the principle is always similar consisting in injecting the selected material (powder, wire, rods) into an area of high temperature where it is melted, accelerated, and directed onto the substrate surface (Ref 1, 2). According to the thermal and kinetic specificities of all processes (APS, VPS, flame, electric arc), all material types can be sprayed provided their melting temperature is at least 300 K lower than their vaporization or decomposition temperature. Among materials, ceramic coatings present several interesting aspects such as wear resistance, corrosion protection as well as thermal or electrical insulation and particularly alumina coatings which appear as the most commonly used.

This article is an invited paper selected from presentations at the 2007 International Thermal Spray Conference and has been expanded from the original presentation. It is simultaneously published in *Global Coating Solutions, Proceedings of the 2007 International Thermal Spray Conference*, Beijing, China, May 14-16, 2007, Basil R. Marple, Margaret M. Hyland, Yuk-Chiu Lau, Chang-Jiu Li, Rogerio S. Lima, and Ghislain Montavon, Ed., ASM International, Materials Park, OH, 2007.

S. Costil, C. Verdy, R. Bolot, and **C. Coddet**, LERMPS-UTBM, 90 010 Belfort cedex, France. Contact e-mail: sophie.costil@utbm.fr.

Many techniques can also be used to spray such kind of materials. Among them, Atmospheric Plasma Spraying (APS) is rather well-established as a commercial process for the deposition of alumina coatings. However, despite the coating microstructures which present typical aspects like inter lamellar micro cracks, unmolten particles, porosities resulting from the rapid solidification of the lamellae, many auxiliary systems are needed to improve the coating characteristics. According to the properties researched, some other processes can also be used and some of them can present a lower economical impact (Ref 3-5). Among them, the flame technology can be employed including rods injection (of alumina) into the energetic source to improve the interaction between the ceramic and the flame (Rokide™, Master Jet®). The energetic content of such flame source being lower than the plasma (when using the APS system), thus the interaction between the ceramic material and the jet is modified. The rods are melted in the spray unit which projects the fully molten particles onto the substrate. All particles must be molten when they leave the rod. These particles have a high kinetic energy and high thermal mass, so they remain molten until they reach the substrate. Moreover, if the alumina particles present a higher cohesive bonding, a lower stress rate can be imagined due to the lower thermal history of the materials. This way, some specific coating microstructures and then some specific coating characteristics can also be deduced.

The aim of this study was to analyze the alumina coating properties according to the technology employed as APS or wire flame spraying using the Rokide™ and the Master Jet® guns. After usual micrographic analyses by SEM, physical and mechanical properties were measured considering the thermal conductivity and hardness. Due to the specific characteristics of such alumina material, it was

interesting to analyze the thermal insulation properties. A numerical model was chosen to estimate this parameter considering two reasons, the results can be obtained faster and no experimental test was available.

2. Experimental Procedure

2.1 Coating Manufacturing and Processing Parameters

The plasma sprayed coatings were deposited using a Sulzer-Metco F4 plasma gun using an Ar/H_2 gas combination and an argon carrier gas flow. A MEDICOAT (MEDICOAT, ETUPES, France) pure alumina powder (Al_2O_3 Medipure), presenting a particle size in the range of 22-45 μm, was chosen as feedstock material. Some specific parameters were applied to deposit the coatings as mentioned in Table 1. Concerning the flame spraying operations, a Retrofit Rokide™ and Master-Jet$_2$® guns, developed by St Gobain (St Gobain Coatings Solutions, Avignon, France), were used. Some sintered pure alumina rods (99.8%, 6.35 mm in diameter, 460 mm in length), were also sprayed. Table 1 summarizes all the specific parameters used to deposit the coatings.

Table 1 Selected processing parameters for the two spraying systems

Atmospheric plasma spraying (APS)	
Arc current intensity, A	600
Argon flow rate, SLPM	46
Hydrogen flow rate, SLPM	14
Feedstock injector diameter, mm	1.8
Feedstock injector tip location from gun centerline axis, mm	6 3.6
Feedstock carrier gas flow rate argon, SLPM	30
Feedstock mass rate, g min^{-1}	125
Spray distance, mm	36
Spray velocity, m min^{-1}	6
Scanning step, mm	
Flame spraying by Rokide™ gun	
Oxygen flow rate, L min^{-1}	36
Oxygen pressure, bars	6.2
Acetylen flow rate, L min^{-1}	23
Acetylen pressure, bars	1.25
Air pressure, MPa	0.6
Feedstock velocity, mm min^{-1}	92
Spray distance, mm	250
Spray velocity, m min^{-1}	6
Scanning step, mm	8
Flame spraying by Master-Jet® gun	
Oxygen flow rate, L min^{-1}	33
Oxygen pressure, bars	5.6
Acetylene flow rate, L min^{-1}	22
Acetylene pressure, bars	1.4
Air pressure, MPa	0.55
Feedstock velocity, mm min^{-1}	90
Spray distance, mm	250
Spray velocity, m min^{-1}	6
Scanning step, mm	8

During the spraying operation, specimens were fixed on a sample holder mounted on the flange of the robot and moved in front of the spraying torch. Of course, several passes in front of the system are necessary to reach the proper coating thickness and adjusted according to the spraying system to obtain 250 μm.

To improve the coating adherence to the substrate, specific steps were carried out on the substrate before spraying. After removing the surface contaminants (by using acetone solution), a grit blasting (using white corundum) of the surface was realized to ensure a surface roughness ($Ra = 2.5$ μm) permitting a mechanical anchorage of the alumina particles on the substrate.

2.2 Coating Structure Characterization

After cutting and infiltrating the samples with epoxy (impregnation technique), they were polished following standard metallographic techniques (pre-polishing and diamond slurry polishing) on an automatic polisher. Samples were observed using SEM (SEM Lov Vaccum, 5800LV, JEOL company) and optical microscopy.

The surface aspect was characterized by roughness measurements (Surtronic 3P-Pick Up 112/1503, Taylor Hobson company) and 15 measures were also realized to estimate the mean roughness (Ra) as well as the Ry_{max}.

2.3 Numerical Computation of the Thermal Conductivity

A numerical code was developed and implemented to numerically estimate the coating thermal conductivity. Analyses were carried out from the coating SEM views constituting a discrete 2-D domain describing the pore and the crack networks (Ref 6-8).

The meshing is directly built from the high-resolution SEM micrograph, where a binary image is obtained after image analysis.

Whatever the coating structure, each pixel of the image corresponds to an element. The method consists also in solving the heat conduction equation by a finite volume method in each pixel of the binary image. Figure 1 shows a schematic representation of the solved problem. To each pixel is attributed the thermal conductivity of the corresponding phase: km for the solid matrix (7.8 W m^{-1} K^{-1} for Al_2O_3 at 1000 K) and kp for air entrapped in porosity (0.03 W.m^{-1} K^{-1}) (Ref 9, 10). Results were also obtained by the temperature value calculated in each pixel of the image inducing the equivalent thermal conductivity corresponding to the considered field. The thermal conductivity of the matrix being dependant on the temperature as reported in the literature (Ref 10), the evolution of the thermal conductivity of the coating has also been calculated.

Calculation results depend nevertheless on the resolution of the SEM views, which reproduce more or less precisely the pore architecture of the coating. Although the different pictures present a similar porosity level, it is obvious that the picture resolution has a significant effect

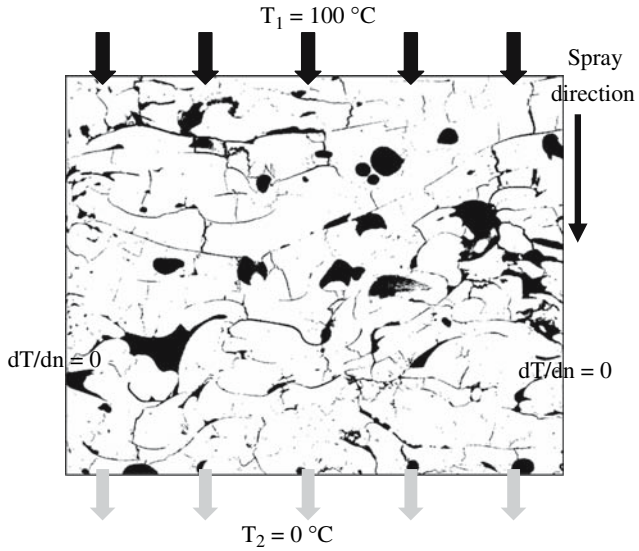

Fig. 1 Problem definition on a binary image of the coating cross section depicting the pore network

on the predicted thermal conductivity. The higher the picture resolution, the lower is the predicted effective thermal conductivity. By decreasing the picture resolution, some pores and interlamellar porosities of the coating microstructure disappear gradually from the image (degradation of the image quality) which improve the simulated propagation of the heat flux across the coating and by this way the thermal conductivity. Then, due to a higher contrast between alumina matrix and porosity (i.e., pores and cracks), backscattered electron mode was chosen preferentially to secondary electron mode.

Magnification level and image resolution were respectively 170*130 μm^2 and 1024*768*8 pixels inducing a physical resolution of 0.17 μm. However, this model presents some limits:

(i) the image resolution is too low to detect the peripheral lamellar decohesions (interlamellar decohesions lower than 0.1 μm) (Ref 11), and hence an overvaluation of the calculated thermal conductivity,

(ii) whatever the dimensions of the pores and micro cracks constituting the coating microstructure, a constant thermal conductivity for the gas was selected (which corresponds to the negligence of the Knudsen effect) (Ref 9),

(iii) the use in calculation of an exclusively two-dimensional method, whereas a three-dimensional effect can exist depending on the geometry and on the orientation of cracks and pores.

Owing to these various uncertainties, the computation results have to be considered indicative rather than exact. In total, 15 calculations were carried out on 15 randomly located images taken on each sample and results were consecutively averaged.

2.4 Coating Mechanical Properties Implementing Knoop Micro-Indentation Test

Selected specimens were also indented using a Knoop hardness tester with a 1.962 N test load on the polished cross sections. Knoop hardness values were considered as an indicator of the coating cohesion, the higher value, the better the cohesion. The longest diagonal of the indenter was aligned parallel to the coating/substrate interface and optical microscopy was used to measure the dimension of the indentation diagonals.

3. Results and Analysis

A specific microstructure of alumina coatings was obtained with the two spraying processes (flame and plasma). Figure 2 illustrates the cross sections of each specimen.

Plasma sprayed coatings appear with a fine microstructure characterized by some micro cracks and pores, whereas coatings deposited by flame processes present bigger architecture. Porosity seems to be more important and some macro cracks can be observed. The surface roughness confirms such tendency as indicated in Table 2.

Even if the melting state of the particles can be assured particularly with the flame process (the alumina material being in a solid state, only the melting part of the rod can be sprayed), some differences concerning the kinetics of the jet in comparison to the plasma jet for example can be put forward as a first explanation.

The interaction between alumina material and the energetic jet (whatever the technology used) seems to be distinctly different. Before impinging the substrate surface, the alumina particles present several characteristics from a kinetic point of view (350 m/s for the particles in the plasma against 220 m/s for the particles in the flame), from the temperature aspect ($T_{max} = 3000$ K in the plasma and $T_{max} = 2700$ K in the flame) as well as considering the particle size ($diam_{max} = 65$ μm when using the flame process, $diam_{max} = 30$ μm when using the plasma process). The larger size of the particles sprayed by the flame process associated to the lower jet properties does not favor the formation of a dense coating. Moreover, some variations can be detected between the two flame processes. Even if the energetic jet is produced in some similar conditions (combustion of a flame), the feedstock of the alumina particles is less regular in the Master Jet® conditions than with the Rokide™ process. In fact, the rod feeding is more precisely defined and adapted with the Rokide™ process to the alumina material in comparison to the Master Jet® technology. More precisely, this last process is defined to spray different kinds of materials from metallics to ceramics contrary to the Rokide™ which was developed specifically for the alumina material. By this way, considering the spray parameters of the oxyde, the rod advance with the Master Jet® is limited in the low range whereas the selected parameters with the Rokide™ torch are in the middle range. Then, the feedstock of the alumina is more regular with the Rokide™ in comparison to the Master Jet®.

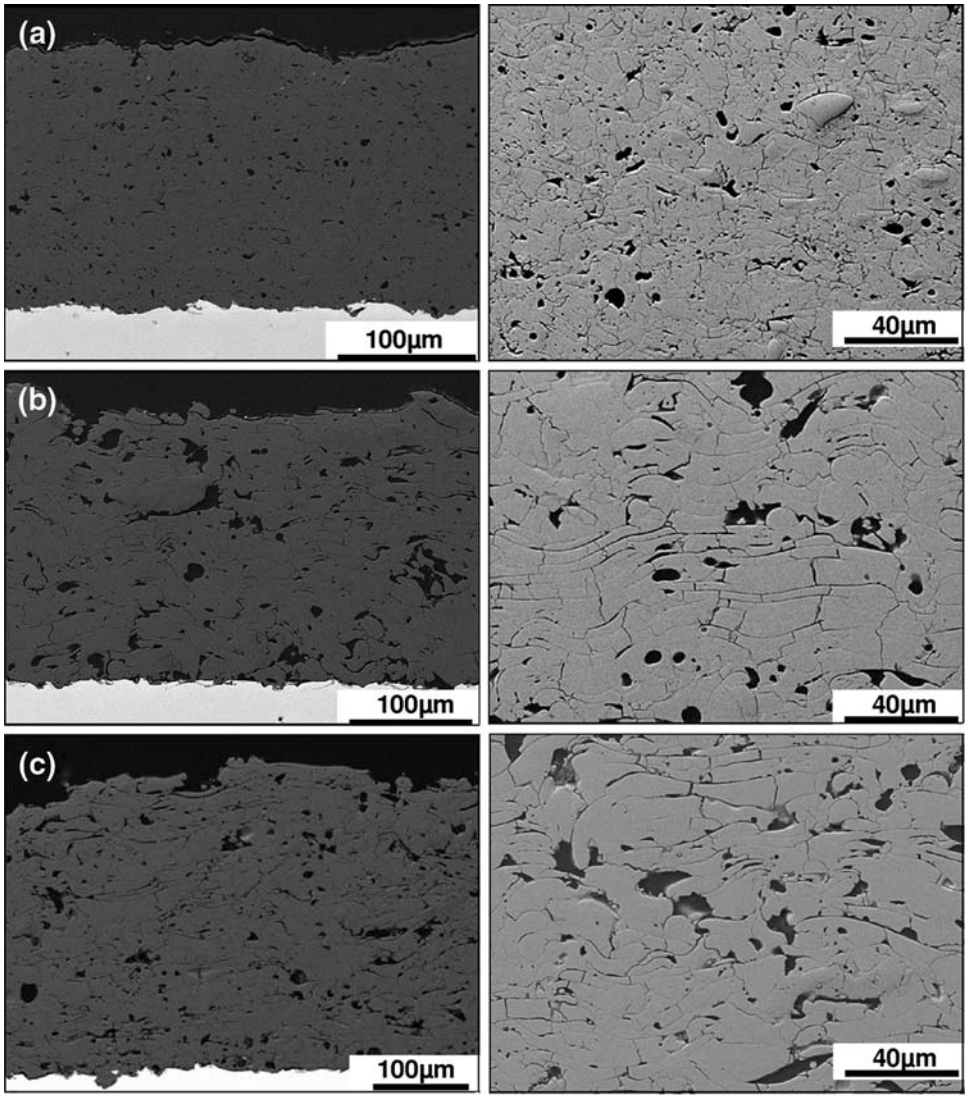

Fig. 2 SEM observations in the cross section of alumina coatings elaborated by: (a) atmospheric plasma spraying (APS), (b) flame spraying using the Rokide™ process, (c) flame spraying using the Master Jet_2® process

Table 2 Roughness characterization of the alumina coatings deposited by all techniques

Processes	*Ra*, µm	Ry_{max}, µm
Coating deposited by APS	4.5 ± 0.3	30.6 ± 2.7
Coating deposited by the Rokide™ process	8.5 ± 0.7	50.3 ± 3.4
Coating deposited by Master Jet_2® process	12 ± 2	79 ± 11

Indeed, such microstructures can be easily correlated to several mechanical or thermal properties. Regarding the cohesion of the coating, the micro-indentation test, performed in order to estimate the average Knoop hardness value, confirms this tendency. Table 3 shows that the coatings elaborated by APS present a higher hardness by about 25% than those sprayed by the flame processes.

Hence, this means that the thinner microstructure induces a better cohesion of the coating than that of Rokide™ or Master Jet® deposits which can be easily confirmed by the variation of the standard deviations too.

Table 3 Results of Knoop micro indentation tests

	Knoop hardness value[a][HK]	Standard deviation
APS coating	800	60
Rokide® coating	580	130
Master Jet™ coating	620	120

[a]Arithmetic average value from 14 adjusted data points

Regarding now thermal conductivity, the same evolution can be noted whatever the coating temperature considered. A higher thermal conductivity was systematically calculated for the coatings elaborated by APS than by flame but lower than bulk alumina (Fig. 3).

This constitutes a promising result and it seems to be linked to the existence of larger cracks in coatings as shown by SEM observations. These cracks appear in the horizontal direction particularly when using the flame

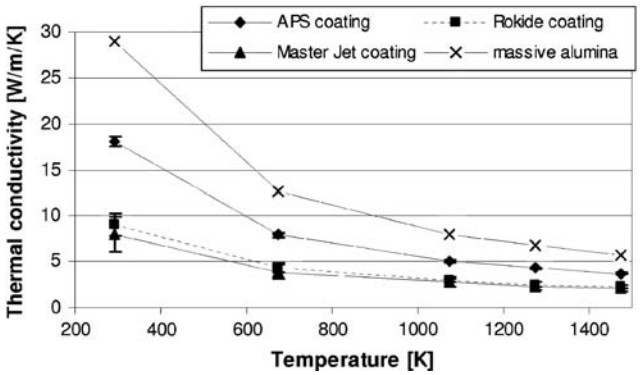

Fig. 3 Evolution of the calculated thermal conductivity as a function of the coating temperature

process. Also, when testing the diffusion of the thermal energy across the coating, its propagation seems to be more affected by the macro cracks (horizontal to the interface) than the inter lamellar micro cracks observed in the APS coatings. The thermal conductivity depends mainly on the true contact between piled-up lamellae. So, those results confirm that the two flame processes improves the thermal insulation of alumina coatings.

This way, it seems that all the variation of the coating characteristics were preferentially linked to the deposition step of the coating. In the case of the flame processes, the large size of the particles before splashing and the low jet properties (lower temperature and speed) did not favor the formation of a dense coating.

4. Conclusion

Several processes can be used to deposit alumina coatings. According to the properties sought for, the choice of a process has to be made. Depending on the process (plasma or flame technologies), the coating characteristics are different. The alumina coatings elaborated by APS technique were denser with a thinner microstructure compared to those sprayed by flame. This way, their mechanical as well as their thermal properties are quite different which can be promising according to the applications.

Acknowledgments

This study was realized with the collaboration of SNECMA. Authors gratefully thank such company as well as St Gobain (and more precisely Mr. P. Fournier) for the availability of the Rokide™ as well as the Master Jet® processes. The authors would like to express their thanks to Ms. F. Moitrier and A. Lidolff for all the works carried out during their training period. LERMPS is member of the *Institut des Traitements de Surface de Franche-Comté* (ITSFC, Surface treatment institute of Franche-Comté), France.

References

1. S. Sampath and H. Herman, Rapid Solidification and Microstructure Development During Plasma Spray Deposition, *J. Therm. Spray Tech.*, 1996, **5**(4), p 445-456
2. P. Fauchais, A. Vardelle, and B. Dussoubs, Quo vadis thermal spraying?, *Proceeding in International Thermal Spray Conference*, C.C. Berndt, K.A. Khor, and E.F. Lugscheider, Eds., ASM international, Materials Park, Ohio, USA, 2001, p 32
3. A. Kulkarni, S. Sampath, A. Goland, H. Herman, and B. Dowd, Computed Microtomography Studies to Characterize Microstructure Property Correlations in Thermal Sprayed Alumina Deposits, *Scipta Mater.*, 2000, **43**, p 471-476
4. R. Yamasaki and J. Takeuchi, Physical Characteristics of Alumina Coating Using Atmospheric Plasma Spraying (APS) and Low Pressure Plasma Spraying (VPS), *Proceeding of the ITSC Conference, Thermal Spray 2004: Advances in technology and application*, A. Ohmori, Ed., May 2004 (Osaka, Japan) ASM International, Materials Park, OH, USA
5. A. Kulkarni, J. Gutleber, S. Sampath, A. Goland, W.B. Lindquist, H. Herman, A.J. Allen, and B. Dowd, Studies of the Microstructure and Properties of Dense Ceramic Coatings Produced by High Velocity Oxygen Fuel Combustion Spraying, *Mater. Sci. Eng.*, 2004, **A369**, p 124-137
6. G. Antou, F. Hlawska, R. Bolot, G. Montavon, C. Coddet, and A. Cornet, Pore Network Architecture and Thermal Conductivity of Y-PSZ TBCs In situ Remelted During Their Deposition, *Proceeding of the ITSC Conference, Thermal Spray Connects: Explore its Surface Potential*, E. Lugscheider, Ed., ASM International, Materials Park, OH, USA, 2005
7. R. Bolot, G. Antou, G. Montavon, and C. Coddet, A Two Dimensional Heat Transfer Model for Thermal Barrier Coating Average Thermal Conductivity Computation, *Numer. Heat Tr. A-Appl.*, 2005, **47**, p 875-898
8. R. Bolot, G. Antou, G. Montavon, and C. Coddet, Calcul numérique de la conductivité thermique des dépôts de zircone yttriée élaborés par projection thermique, *Proceeding of Matériaux 2006 Conference*, Dijon, France, novembre 2006
9. E. Litovsky, M. Shapiro, and A. Shavit, Gas Pressure and Temperature Dependences of Thermal Conductivity of Porous Ceramics Materials: Part I, Refractories and Ceramics with Porosity Below 30%, *J. Am. Ceram. Soc.*, 1992, **75**(12), p 3425-3439
10. M. Laurent and P.L. Vuillermoz, Conductivité thermmique des solides (in french), *Techniques de l'ingénieur*, K420, p 1-29
11. L. Bianchi, P. Lucchese, A. Denoirjean, and P. Fauchais, Microstructural Investigation of Plasma Sprayed Alumina Splats, NTSC95, *Proceeding of thermal spray science and technology*, C.C. Berndt, Ed., ASM International, Materials Park, OH, USA, 1995, p 255-260